Magnetic pair breaking and weak ferromagnetism in single crystals of $Er_{1-x}Tb_xNi_2B_2C$

Chang-An Kim and B. K. Cho*
Center for Frontier Materials, Department of Materials Science and Engineering, Kwangju Institute of Science and Technology, Gwangju 500-712, Korea

(Received 11 July 2002; published 6 December 2002)

The magnetic and superconducting properties in the single crystals of $Er_{1-x}Tb_xNi_2B_2C$ compounds are investigated by temperature-dependent magnetization $M(T)$ and in-plane resistivity $\rho(T)$. It is found that the superconducting transition temperature is suppressed by adding Tb in the sites of Er and it follows well de Gennes scaling for both $T_c > T_N$ and $T_c < T_N$. From the T_c variation, the magnetic pair breaking strength of Tb is estimated to be similar to the Er. The antiferromagnetic and weak ferromagnetic transition temperatures show distinct behaviors in terms of the de Gennes factor in the Er-rich ($x \leqslant 0.4$) and Tb-rich ($x \geqslant 0.6$) side. These observations will be discussed under the consideration of magnetic ground states of $ErNi_2B_2C$ and $TbNi_2B_2C$ and their interactions.

DOI: 10.1103/PhysRevB.66.214501 PACS number(s): 74.25.Ha, 74.70.Dd

I. INTRODUCTION

Since the discovery of quaternary compound of RNi_2B_2C (R=Y, and rare-earth elements), much attention has been focused on the interaction between superconductivity and magnetism as well as superconductivity itself.[1] Among them, $ErNi_2B_2C$ shows superconducting transition at $T \approx 11$ K, antiferromagnetic order below $T_N \approx 6$ K with transverse incommensurating modulation vector $\delta_{Er} = (0.5526, 0, 0)$, and weak ferromagnetic component below $T \approx 2$ K.[2,3] The coexistence of superconductivity and weak ferromagnetism revitalized the interests on the self-induced vortex states, which has long been predicted but not observed yet in a ferromagnetically ordered superconductors.[4] In addition, a large enhancement of the critical currents is observed for all field orientations in the ferromagnetic regime, corresponding to an increase of the pinning force of the flux lattice, probably due to strong pair breaking by the ferromagnetism.[5] The nonsuperconducting $TbNi_2B_2C$ compound exhibits the similar magnetic structure to the one of $ErNi_2B_2C$ below $T_N \approx 15$ K involving an incommensurate antiferromagnetic modulation, which can be described as a longitudinally polarized spin-density wave vector $\delta_{Tb} = (0.555, 0, 0)$.[2] Neutron-diffraction and magnetization studies have revealed weak ferromagnetic component below $T_{WF} \approx 8$ K, whereas other report proposed a small ferromagnetic component along with antiferromagnetic ordering even at $T \approx 15$ K.[6,8]

Based on the magnetic similarity in the magnetic structure and difference in the modulation vector between $ErNi_2B_2C$ and $TbNi_2B_2C$, the study of $Er_{1-x}Tb_xNi_2B_2C$ system is interesting in terms of both magnetism and superconductivity. It may be possible to increase the T_{WF} by replacing the Er elements with Tb to enhance the effects of the weak ferromagnetic component. It is shown that the superconducting T_cs of the RNi_2B_2C (R=Lu, Y, Tm, Er, Ho, and Dy) are not on an universal curve of Abrikosov-Gor'kov theory, indicating that each rare-earth element has different magnetic pair breaking strength probably due to the microscopic magnetic state caused by crystalline electric-field effect. The T_c variation in the $Er_{1-x}Tb_xNi_2B_2C$ system will be compared with the other systems to discuss the magnetic pair breaking effects. So far, all of the studies of the $Er_{1-x}Tb_xNi_2B_2C$ compounds are performed with polycrystalline samples and discrepancies exist between them.[9–11] It is also shown that the sample homogeneity significantly affects the superconducting properties. Therefore it is worthwhile to study the $Er_{1-x}Tb_xNi_2B_2C$ compounds in a high quality single crystalline form.

II. EXPERIMENT

The single crystals of $Er_{1-x}Tb_xNi_2B_2C$ were synthesized by using high-temperature metal flux method as described elsewhere.[12] The powder x-ray-diffraction patterns of pulverized single crystals is nicely indexed in terms of tetragonal lattice structure with $I4/mmm$ symmetry group, indicating single phase without noticeable impurities. It is found that the grown crystals are platelike and the c axis of the single crystals is normal to their flat surfaces. dc magnetization measurements are performed with the applied field parallel to the ab plane by using a superconducting quantum interference device (SQUID) magnetometer (Quantum Design MPMS). The zero-field electrical resistivity is measured by standard four-probe method under the temperature and field control of the SQUID. The contact resistance is lowered below 1 Ω.

III. RESULTS AND DISCUSSION

The temperature-dependent resistivity $\rho(T)$ and magnetization divided by applied field $M(T)/H$ were measured for the single crystals of $Er_{1-x}Tb_xNi_2B_2C$ (x=0.0, 0.1, 0.2, 0.25, 0.3, 0.35, 0.4, 0.6, 0.7, 0.8, 0.9, and 1.0) in order to study the superconductivity, magnetism and their interplay in the temperature range of $2 \leqslant T \leqslant 20$ K. As a representative data set, the $\rho(T)$ and $M(T)$ for $Er_{1-x}Tb_xNi_2B_2C$ (x =0.25) are plotted in Fig. 1(a). Figure 1(b) shows a temperature derivative of the $M(T)$ and a expanded plot for the $\rho(T)$ of Fig. 1(a). The $\rho(T)$ is measured in zero applied field and the $M(T)$ is done under H=100 G, perpendicular to the crystallographic c axis. The antiferromagnetic transition,

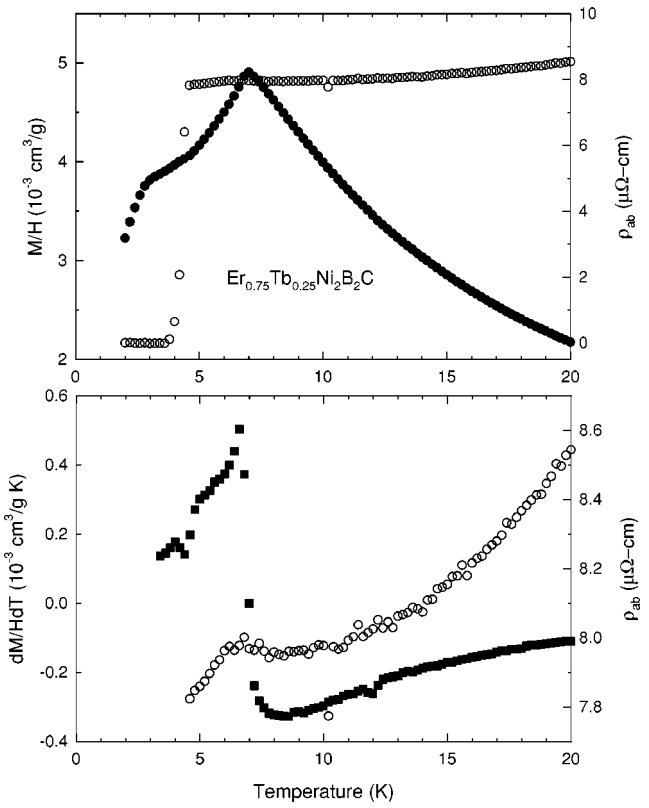

FIG. 1. (a) Temperature-dependent magnetization divided by magnetic field M/H (filled circles) and in-plane resistivity ρ_{ab} (open circles) of $Er_{0.75}Tb_{0.25}Ni_2B_2C$, and (b) temperature derivative of the magnetization (filled squares) and expanded plot of the ρ_{ab}.

which was found in $ErNi_2B_2C$ and $TbNi_2B_2C$, is manifested itself as the peak in the $M(T)$ near $T=7$ K and the Néel temperature T_N is defined as the temperature of the peak in the temperature derivative of $M(T)$ as in Fig. 1(b). The zero-field resistivity represents superconducting transition at $T=4$ K as a zero resistivity temperature in Fig. 1(a). So, the sudden drop of the magnetization near $T=2$ K is due to the superconducting diamagnetic signal where the superconducting transition is suppressed by the external applied field. The antiferromagnetic transition, found in the $M(T)$, is also manifested as a kink in the expanded plot of the $\rho(T)$ in Fig. 1(b), of which the temperature nicely coincides with the T_N defined in the temperature derivative of $M(T)$ data. Since the similar behavior of $M(T)$ and $\rho(T)$ for superconducting and antiferromagnetic transition is observed for the specimens of $Er_{1-x}Tb_xNi_2B_2C$ with $x=0.2$, 0.3, 0.35, 0.4, it is straightforward to find the superconducting transition temperatures and Néel temperatures for these compounds.

Figure 2 shows the $M(T)/H$ and $\rho(T)$ data for $Er_{1-x}Tb_xNi_2B_2C$ ($x=0.3$) with the same measurement conditions as in Fig. 1. It represents the antiferromagnetic transition in $M(T)$ and superconducting transition near $T=2$ K. It should be noted that the $M(T)$ data below T_N does not show the reduction of magnetization due to superconducting diamagnetic signal as seen in Fig. 1 but rather a slight increase at the lowest temperature available. This low-temperature upturn of the $M(T)$ is observed for the single

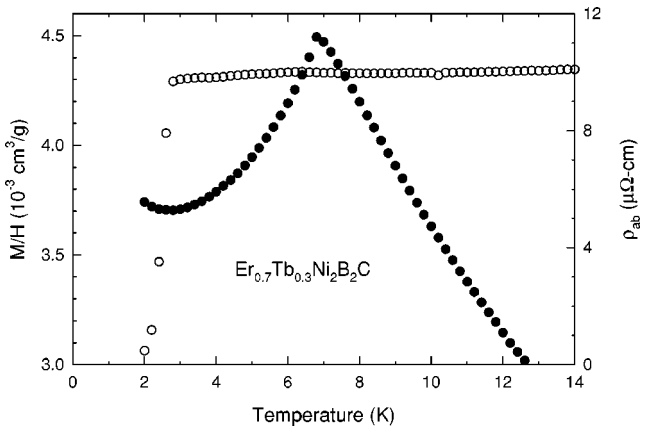

FIG. 2. Temperature-dependent magnetization divided by magnetic field M/H (filled squares) and in-plane resistivity ρ_{ab} (open circles) of $Er_{0.7}Tb_{0.3}Ni_2B_2C$.

crystals with the value of $0.3\leqslant x\leqslant 1.0$. Considering the high quality of single crystals and weak ferromagnetic signals in $ErNi_2B_2C$,[3] $TbNi_2B_2C$,[7] and $Y_{1-x}Tb_xNi_2B_2C$,[13] the upturn signal of $M(T)$ at low temperature may be an indication of an uncompensated magnetic moment. It would be of great interest to investigate magnetization below $T=2$ K.

For the case of $Er_{1-x}Tb_xNi_2B_2C$ ($x=0.6$), the antiferromagnetic transition in $M(T)$ cannot be defined as clear as for $x=0.25$ in Fig. 1 as seen in Fig. 3. A plateau region, rather than a peak, appears below the paramagnetic region with decreasing temperature and an upturn of $M(T)$ with further decreasing temperature. The temperature derivative of the magnetization cannot be used to define the Néel temperature in these data. The upturn of the $M(T)$ at low temperatures is an indication of weak ferromagnetism. The resistivity for the same sample shows metallic behavior down to $T=12$ K, upturn for $12\geqslant T\geqslant 9$ K, and decreases again below 9 K. It is likely that the upturn for $12\geqslant T\geqslant 9$ K is due to the magnetic fluctuation near the long-range ordering and the decrease below $T=9$ K is due to the loss of magnetic scattering below antiferromagnetic (AF) ordering. Since the resistivity onset of magnetic scattering loss in Fig. 1(b) is found to coincide

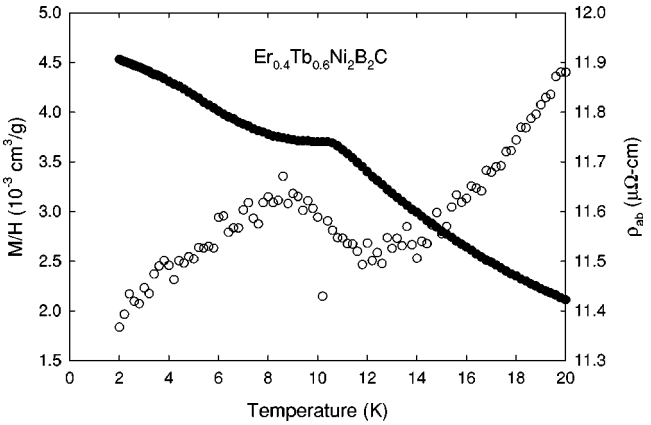

FIG. 3. Temperature-dependent magnetization divided by magnetic field M/H (filled squares) and in-plane resistivity ρ_{ab} (open circles) of $Er_{0.4}Tb_{0.6}Ni_2B_2C$.

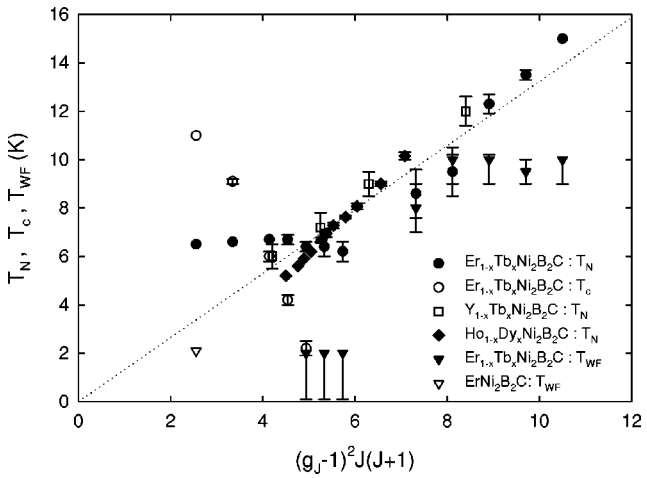

FIG. 4. Antiferromagnetic transition temperature T_N, superconducting transition temperature T_c, and weak ferromagnetic temperature T_{WF}, versus de Gennes value $(g_J-1)^2J(J+1)$ for various compounds. $Er_{1-x}Tb_xNi_2B_2C$: this work; $Y_{1-x}Tb_xNi_2B_2C$: Ref. 13; $Ho_{1-x}Dy_xNi_2B_2C$: Ref. 14; and $ErNi_2B_2C$: Ref. 3.

with the Néel temperature defined by the temperature derivative of $M(T)$, the Néel temperatures for $x \geqslant 0.6$ can be defined as the sudden slope change of the $\rho(T)$ data. The resistivity increases due to the magnetic fluctuation for $12 \geqslant T \geqslant 9$ K are largest among the samples studied in this work. This indicates that the magnetic correlation between the two magnetic sites of Er and Tb is relatively weak.

The superconducting and magnetic phase diagram in terms of effective de Gennes (DG) factor, determined from $M(T)$ and $\rho(T)$ data, are plotted in Fig. 4. There is almost no change of T_N for the samples of $Er_{1-x}Tb_xNi_2B_2C$ with $x \leqslant 0.4$ and the T_N follows DG values for $x \geqslant 0.6$. The suppression of the T_c with respect to the DG values is seen as expected by Abrikosov-Gor'kov (AG) theory that describes the magnetic effect on the superconductivity in terms of the exchange interaction between the magnetic moments and conduction electrons. The crossover for $T_c < T_N$ is observed in the sample with $x=0.2$ and the AG scaling of the T_c is still valid even for the temperatures of $T_c < T_N$, contrary to the case of $Ho_{1-x}Dy_xNi_2B_2C$ where the T_c is independent of DG values for $T_c < T_N$.[14] The observed variations of T_c and T_N are consistent with the ones in Ref. 11. However, the superconductivity is observed even for $x=0.3$, which is the largest Tb concentration compared with $x=0.2$ in Ref. 9 and $x=0.25$ in Ref. 11. This indicates a high homogeneity of single phase in our single crystals. In addition, we are able to identify the weak ferromagnetic signal in the Er-rich side of the samples as a slight increase of magnetization near $T=2$ K.

In order to understand the magnetic interactions, the T_N versus DG values for the single crystalline samples of $Y_{1-x}Tb_xNi_2B_2C$,[13] and $Ho_{1-x}Dy_xNi_2B_2C$,[14] are also plotted in Fig. 4. The dotted line in Fig. 4 is a theoretical DG scaling of T_N based on the Ruderman-Kittel-Kasuya-Yosida (RKKY) interaction between the magnetic moments. As can be seen, the T_N's of the compounds of $Y_{1-x}Tb_xNi_2B_2C$ and $TmNi_2B_2C$, which contains only one kind of magnetic ions, follows well the DG scaling as expected. The compounds of $Ho_{1-x}Dy_xNi_2B_2C$, $Er_{1-x}Tb_xNi_2B_2C$, containing two kinds of magnetic ions, reveals different DG scaling, where the $Ho_{1-x}Dy_xNi_2B_2C$ shows simple DG scaling for the whole series and the $Er_{1-x}Tb_xNi_2B_2C$ abnormal behavior. This different behavior can be understood by considering the magnetically ordered structure of each compound. Because the $HoNi_2B_2C$ and $DyNi_2B_2C$ have the same magnetic structure below T_N, the mixing of the two magnetic ions of Ho and Dy will not change the magnetic interaction strength between them and result in normal DG scaling. However, the magnetic structures of $ErNi_2B_2C$ and $TbNi_2B_2C$ are not the same below T_N in terms of the modulation vector. If the interaction between the Er and Tb is relatively weak as mentioned above, the interaction between the same kinds of ions will determine the T_N variation. The Tb-rich side of $Er_{1-x}Tb_xNi_2B_2C$ will follow the DG expectation as in $Y_{1-x}Tb_xNi_2B_2C$. On the other hand, the T_N values in the Er-rich side of $Er_{1-x}Tb_xNi_2B_2C$ will move toward the one of $ErNi_2B_2C$, which is higher than the DG expectation probably due to microscopic magnetic anisotropy.

The weak ferromagnetic temperatures T_{WF} can be also accounted for in the two different regions, i.e., Er-rich and Tb-rich regions. The T_{WF} in the Er-rich region is almost constant at $T \approx 2$ K, which is same as the one for $ErNi_2B_2C$.[3] The T_{WF} in the Tb-rich region moves around $T=8 \sim 10$ K with increasing Tb concentration. The two different natures of weak ferromagnetic state are manifested themselves in the magnetization data at low temperatures as seen in Figs. 2 and 3. Because the interaction between the two magnetic sites of Er and Tb is relatively weak, no enhancement of T_{WF} in the superconducting state by replacing Er with Tb elements is observed in the Er-rich side of the $Er_{1-x}Tb_xNi_2B_2C$ system. For the Tb-rich side of the same samples, the T_{WF} jumps to around 9 K, similar to the T_{WF} of pure $TbNi_2B_2C$.

The normalized superconducting transition temperatures for various samples of single crystals are plotted versus DG values in Fig. 5. As can be seen, the normalized T_c's are not on a universal curve for the DG scaling. This means that each magnetic element has a different magnetic strength as a superconducting pair breaker. This fact is probably due to the magnetic anisotropy caused by the crystalline electric-field (CEF) effect and due to the microscopic magnetic interaction, leading to the different magnetic structures below T_N. Because the Gd ion is free from the CEF effect and, consequently, shows an isotropic three-dimensional magnetic nature, the data of the $Y_{1-x}Gd_xNi_2B_2C$ system can be considered as a universal one based on the AG theory.[14] Other magnetic elements, such as Er, Ho, Tb, Dy, which show a two-dimensional magnetic state, exhibit less effective pair breaking than Gd. It is obvious that Er and Tb have similar effects on the superconductivity. It is quite interesting to notice that the ground-state magnetic structures of the both $ErNi_2B_2C$ and $TbNi_2B_2C$ below T_N consist of AF layers perpendicular to the c axis and the ones of the both $HoNi_2B_2C$ and $DyNi_2B_2C$ of alternating ferromagnetic layers.[2] The difference of $ErNi_2B_2C$ and $TbNi_2B_2C$ is in the direction of modulation vector of the magnetic moments,

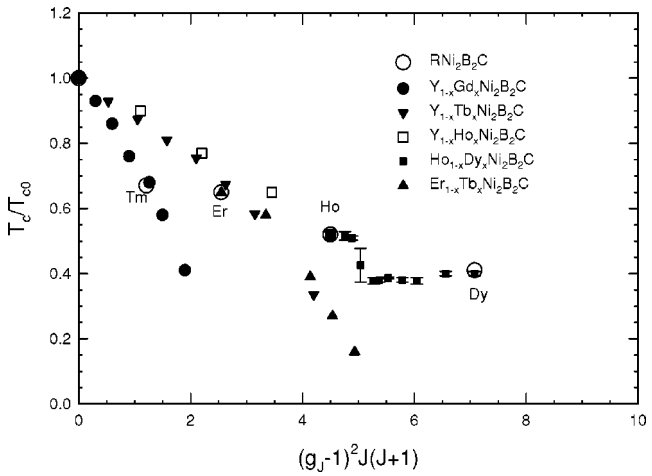

FIG. 5. Normalized superconducting transition temperature versus de Gennes value, $(g_J-1)^2J(J+1)$, for various compounds. $Er_{1-x}Tb_xNi_2B_2C$: this work; $Y_{1-x}Tb_xNi_2B_2C$: Ref. 13; $Ho_{1-x}Dy_xNi_2B_2C$, $Y_{1-x}Ho_xNi_2B_2C$, $Y_{1-x}Gd_xNi_2B_2C$: Ref. 14; and RNi_2B_2C: Ref. 1.

which is perpendicular to the AF ordering axis in $ErNi_2B_2C$ and parallel to the AF ordering axis in $TbNi_2B_2C$. Therefore it seems that the anisotropic magnetic interaction within the ordering plane even above T_N has a clear effect on the strength of magnetic pair breaking.

As mentioned above, the T_c's for $T_c<T_N$ in $Er_{1-x}Tb_xNi_2B_2C$ follow AG expectation while the ones in $Ho_{1-x}Dy_xNi_2B_2C$ are independent of the DG factor. Recently, the abnormal behavior of the T_c of $Ho_{1-x}Dy_xNi_2B_2C$ for $T_c<T_N$ is explained in terms of the cancellation of effective magnetic field at the Ni site by considering the symmetry of magnetic structure below T_N.[15] This phenomenological model is suitable in the $Ho_{1-x}Dy_xNi_2B_2C$ system because the two compounds of $HoNi_2B_2C$ and $DyNi_2B_2C$ have exactly same magnetic ground structures. However, this model cannot be applied to the $Er_{1-x}Tb_xNi_2B_2C$ system, studied in this paper, because the two compounds of $ErNi_2B_2C$ and $TbNi_2B_2C$ have different magnetic modulation vectors, resulting in no perfect cancellation of the effective magnetic field at Ni site. This behavior is also consistent with the fact that the magnetic interaction between Er and Tb is relatively weak.

IV. CONCLUSION

The series of $Er_{1-x}Tb_xNi_2B_2C$ compounds exhibits variety of magnetism, superconductivity, which were seen in $ErNi_2B_2C$ and $TbNi_2B_2C$, and the interplay between them. The T_c of $ErNi_2B_2C$ is suppressed by adding a Tb element and a crossover for $T_c<T_N$ occurs at $x=0.2$. The T_c variation follows well the DG scaling down to $T_c\approx 2$ K and $x=0.3$ contrary to $Ho_{1-x}Dy_xNi_2B_2C$. From the T_c variation, it is conjectured that the magnetic pair breaking strength of Tb in RNi_2B_2C compounds is comparable with Er probably because of the similar magnetic interaction, leading to the compensated magnetic layer perpendicular to the c axis below T_N. However, the difference in terms of the modulation vectors is likely to cause a weak interaction between the Er and Tb in $Er_{1-x}Tb_xNi_2B_2C$, leading to distinct T_N and T_{WF} variation with the DG values in Er- and Tb-rich compounds. This means that the observed magnetic subtle effects should be included to make microscopic corrections in the AG theory and magnetic interactions.

ACKNOWLEDGMENTS

This work was supported by a Korea Research Foundation Grant (KRF-2002-070-C00032).

*Email address: chobk@kjist.ac.kr

[1] P.C. Canfield, P.L. Gammel, and D.J. Bishop, Phys. Today **51** (10), 40 (1998).
[2] J.W. Lynn, S. Skanthakumar, Q. Huang, S.K. Sinha, Z. Hossain, L.C. Gupta, R. Nagarajan, and C. Godart, Phys. Rev. B **55**, 6584 (1997).
[3] P.C. Canfield, S.L. Bud'ko, and B.K. Cho, Physica C **262**, 249 (1996).
[4] T.K. Ng and C.M. Varma, Phys. Rev. Lett. **78**, 330 (1997).
[5] P.L. Gammel, B. Barber, D. Lopez, A.P. Ramirez, D.J. Bishop, S.L. Bud'ko, and P.C. Canfield, Phys. Rev. Lett. **84**, 2497 (2000).
[6] P. Dervenagas, J. Zarestky, C. Stassis, A.I. Goldman, P.C. Canfield, and B.K. Cho, Phys. Rev. B **53**, 8506 (1996).
[7] B.K. Cho, P.C. Canfield, and D.C. Johnston, Phys. Rev. B **53**, 8499 (1996).
[8] C.V. Thomy, L.J. Chang, D.McK. Paul, and C. Ritter, Physica B **230-232**, 872 (1997).
[9] A. Rustom, A.D. Hillier, and R. Cywinski, J. Magn. Magn. Mater. **177-181**, 1153 (1998).
[10] Z.Q. Peng, K. Krug, and K. Winzer, Physica C **317-318**, 441 (1999).
[11] H. Bitterlich, W. Loser, G. Behr, K. Nenkov, G. Fuchs, A. Gumbel, and L. Schultz, Physica C **321**, 93 (1999).
[12] B.K. Cho, P.C. Canfield, L.L. Miller, D.C. Johnston, W.P. Beyermann, and A. Yatskar, Phys. Rev. B **52**, 3684 (1995).
[13] B.K. Cho, H.B. Kim, and S.I. Lee, Phys. Rev. B **63**, 144528 (2001).
[14] B.K. Cho, P.C. Canfield, and D.C. Johnston, Phys. Rev. Lett. **77**, 163 (1996).
[15] H. Doh, M. Sigrist, B.K. Cho, and Sung-Ik Lee, Phys. Rev. Lett. **83**, 5350 (1999).